Bull. Chem. Soc. Ethiop. **2013**, 27(2), 315-319.
Printed in Ethiopia
DOI: http://dx.doi.org/10.4314/bcse.v27i2.18
ISSN 1011-3924

SHORT COMMUNICATION

PHOTOLUMINESCENCE PROPERTIES OF THE RED PHOSPHOR $YInGe_2O_7:Eu^{3+}$

Jianpeng Han[1], Liya Zhou[1,*], Qi Pang[2,*] and Hong Yang[1]

[1]School of Chemistry and Chemical Engineering, Guangxi University, Nanning, 530004, China
[2]Department of Chemistry and Biology, Yulin Normal University, Yulin, 537000, China

(Received October 31, 2011; revised January 8, 2013)

ABSTRACT. Eu^{3+}-doped $YInGe_2O_7$ phosphors were prepared via a solid-state reaction with metal oxides and their excitation and emission spectra were measured at room temperature. The results showed that pure-phase $YInGe_2O_7$ could be obtained after firing at 1250 °C. The maximum photoluminescence intensity of $YInGe_2O_7:Eu^{3+}$ phosphor was achieved when doped with 40 mol% Eu^{3+} ions. Compared with $Y_2O_2S:0.05Eu^{3+}$, the $Y_{0.60}InGe_2O_7:Eu^{3+}_{0.40}$ phosphor obtained showed intense red-emission lines at 616 nm, corresponding to forced electric dipole $^5D_0 \rightarrow {}^7F_2$ transitions of Eu^{3+} under 394 nm light excitation. The International Commission on Illumination chromaticity coordinates of the phosphors (x = 0.644, y = 0.356) of $Y_{0.60}InGe_2O_7:Eu^{3+}_{0.40}$ were close to National Television Standard Committee standard values. As such, the synthesized phosphors may find applications in near ultraviolet InGaN chip-based white light-emitting diodes.

KEY WORDS: Optical materials, X-Ray diffraction, Luminescence, Solid state reaction

INTRODUCTION

White light emitting diodes (LEDs) feature high efficiency, reliability, rugged construction, low power consumption, and durability; as such, they are called next generation solid-state lights [1–4]. Considering that oxide phosphors have higher chemical stability than sulfide phosphors, many studies have been conducted to develop new oxide phosphors that are suitable for many applications such in field emission displays and white LEDs [5–10].

Yttrium indium germinate has the symmetrical structure of the $C_{2/m}$ space group with a thortveitite structure. Y^{3+} and In^{3+} cations occupy the same octahedral site and the InO_6/YO_6 octahedral layers are held together to form a hexagonal arrangement. In this compound, the Ge_2O_7 diorthogroup shows C_{2h} symmetry, implying that the Ge–O–Ge angle is 180° [11, 12]. $YInGe_2O_7$ has been suggested to be a favorable candidate host material for phosphors. The efficiency of phosphors is often limited by the dynamics of the dopant ion, the properties of which depend on interactions with the host materials.

Eu^{3+}-doped phosphors that emit bright red light have been widely used in many fields [13–16]. Eu^{3+} exhibits different optical properties in various host lattices due to changes in the surrounding environment. In this paper, $YInGe_2O_7:Eu^{3+}$ phosphors were prepared by the solid-state reaction method and then characterized. The luminescent properties of the phosphors were also investigated.

EXPERIMENTAL

The preparation of phosphors. $YInGe_2O_7:Eu^{3+}$ samples were prepared by the solid-state reaction method using Y_2O_3 (99.99%), GeO_2 (99.99%), and Eu_2O_3 (99.99%) powders. Stoichiometric amounts of starting materials were mixed homogeneously in an agate mortar and calcined in air at 1100, 1200, 1250, and 1300 °C for 5 h.

*Corresponding author. E-mail: zhouliyatf@163.com

Y_2O_2S:0.05Eu^{3+} phosphors were prepared according to Ref. [17]. The starting materials Y_2O_3, Eu_2O_3, S, and Na_2CO_3 were ground and then fired at 1100 °C in a CO-reducing atmosphere. After annealing, the samples were washed with dilute nitric acid and deionized water and then dried at 100 °C. The X-ray powder diffraction (XRD) pattern of Y_2O_2S:0.05Eu^{3+} is shown in Figure 1(e).

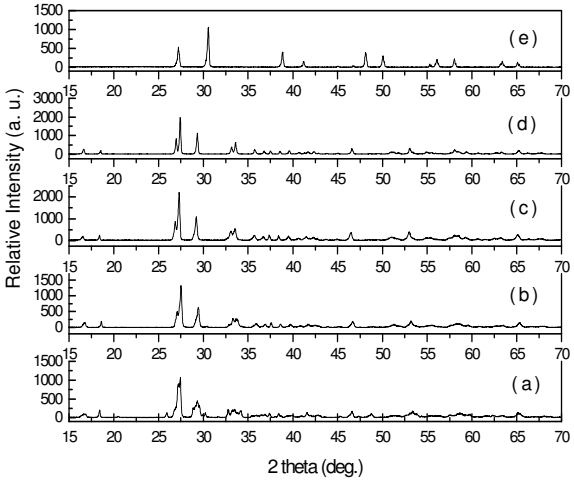

Figure 1. XRD patterns of the $Y_{0.95}InGe_2O_7$:$Eu^{3+}_{0.05}$ phosphor calcined at (a) 1100 °C, (b) 1200 °C, (c) 1250 °C, (d) 1300 °C and the XRD patterns of Y_2O_2S:0.05Eu^{3+}(e), respectively.

Characterization. The structure of the samples was examined by XRD (40 kV and 200 mA, Cu $K\alpha$ = 1.5406 Å, Rigaku/Dmax – 2500). A laser nanometer granulometer (Zetasizer Nano S) was used to observe the distribution and size of the particles. The excitation and emission spectra were recorded on an F-2500 fluorescence spectrophotometer with a Xe lamp as the excitation source. All of the measurements were conducted at room temperature.

RESULTS AND DISCUSSION

X-ray diffraction and size distribution characterization. The XRD patterns of $YInGe_2O_7$ doped with 5 mol% Eu^{3+} show the formation of a crystalline phase, as illustrated in Figures 1a–1d. The crystalline phase, which features a monoclinic structure, appears at 1100 °C, and the doped Eu^{3+} ion has little influence on the host structure [11, 12]. When the firing temperature is increased from 1100 °C to 1300 °C, the peak widths decrease and the peak intensities strengthen because of the increased crystallinity. Eu^{3+} ions (0.95 Å) are introduced to substitute the Y^{3+} ions (0.9Å) in $YInGe_2O_7$ [18]. Figure 2 shows the particle size distribution of the $Y_{0.95}InGe_2O_7$:$Eu^{3+}_{0.05}$ phosphor calcined at 1250 °C. The particles show a narrow size distribution. The average diameter of the particles is about 3 μm to 4 μm.

Photo-luminescent properties. Figure 3 shows the excitation and emission spectra of the $Y_{0.95}InGe_2O_7$:$Eu^{3+}_{0.05}$ samples fired at 1250 °C. During monitoring of the emission at 616 nm, the excitation spectrum of $Y_{0.95}InGe_2O_7$:$Eu^{3+}_{0.05}$ exhibits a wide band in the ultraviolet (UV) region centered at approximately 260 nm, which is ascribed to ligand-to-Eu^{3+} charge transfer transitions [19]. The sharp lines in the 360 nm to 500 nm range indicate the intra-configurational 4f–4f transitions of Eu^{3+} in the host lattices, and the strong excitation bands at 394 and 464 nm are attributed to the $^7F_0 \rightarrow {}^5L_6$ and $^7F_0 \rightarrow {}^5D_2$ transitions of Eu^{3+}, respectively.

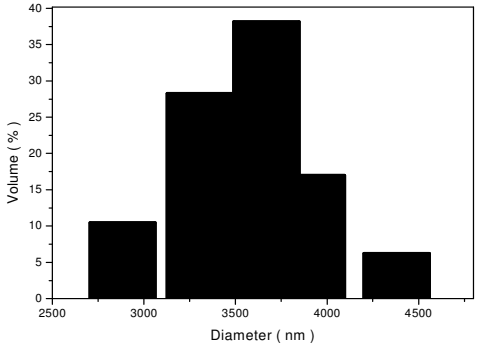

Figure 2. Particle size distribution of $Y_{0.95}InGe_2O_7:Eu^{3+}{}_{0.05}$ phosphor calcined at 1250 °C.

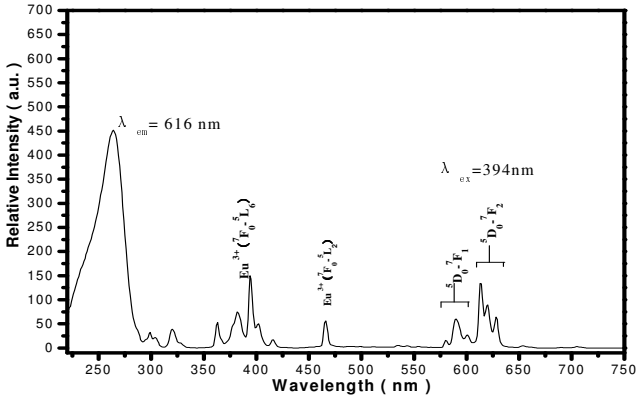

Figure 3. UV excitation (λ_{em} = 616 nm) and emission (λ_{ex} = 394 nm) spectra of $Y_{0.95}InGe_2O_7:Eu^{3+}{}_{0.05}$ phosphors fired at 1250 °C.

Upon excitation with 394 nm UV irradiation, the emission spectra are described by the well-known $^5D_0 \rightarrow {}^7F_J$ (J = 0, 1, 2, etc.) emission lines of Eu^{3+} ions, which have strong emission at J = 2 and 616 nm, thereby allowing the ions to occupy a center of asymmetry in the host lattice. The ratio of the integrated intensities of these two transitions, I_{0-2}/I_{0-1}, is used in lanthanide-based systems as a probe for the local surroundings of cations [20]. As shown in Figure 2, the $^5D_0 \rightarrow {}^7F_2$ transition is much stronger than the $^5D_0 \rightarrow {}^7F_1$ transition, which suggests that Eu^{3+} is located in a distorted (or asymmetric) cation environment. Other transitions, such as those of $^5D_0 \rightarrow {}^7F_1$, $^5D_0 \rightarrow {}^7F_3$, and $^5D_0 \rightarrow {}^7F_4$, located at the 570 nm to 750 nm range are relatively weak, which is advantageous for obtaining saturated International Commission on Illumination (CIE) chromaticity. The CIE chromaticity coordinates of the phosphor $Y_{0.60}InGe_2O_7:Eu^{3+}{}_{0.40}$ are calculated to be x = 0.644, y = 0.356, close to the National Television Standard Committee (NTSC) standards (x = 0.670, y = 0.330). The effect of the doped-Eu^{3+} content of the $Y_{1-x}InGe_2O_7:Eu^{3+}{}_x$ phosphors calcined at 1250 °C on the relative photoluminescence (PL) intensity at the highest $^5D_0 \rightarrow {}^7F_2$ transition is shown in Figure 4. All of the $Y_{1-x}InGe_2O_7:Eu^{3+}{}_x$ phosphors show similar PL spectra excluding their relative intensity. The PL emission intensity increases with increasing Eu^{3+} doping ratio and achieves a maximum value at x = 0.40. However, when the Eu^{3+} doping ratio is above 40 mol%, the luminescence intensity decreases. This quenching process is often attributed to energy migration among Eu^{3+} ions.

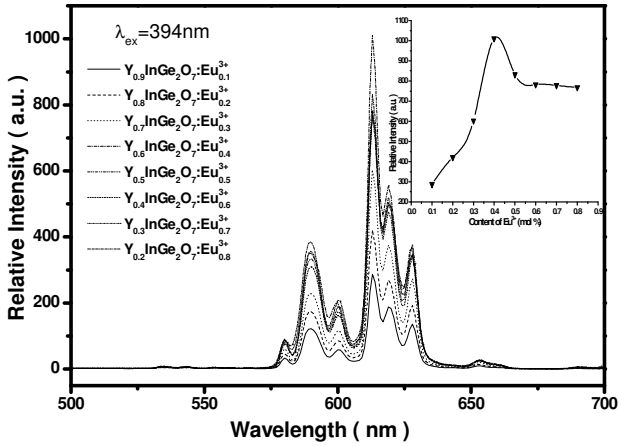

Figure 4. Emission (λ_{ex} = 394 nm) spectra of $Y_{1-x}InGe_2O_7:Eu^{3+}{}_x$ phosphors with different Eu^{3+} doping ratios. Inset: detail of the effect of the doped-Eu^{3+} content in $Y_{1-x}InGe_2O_7:Eu^{3+}{}_x$ phosphors.

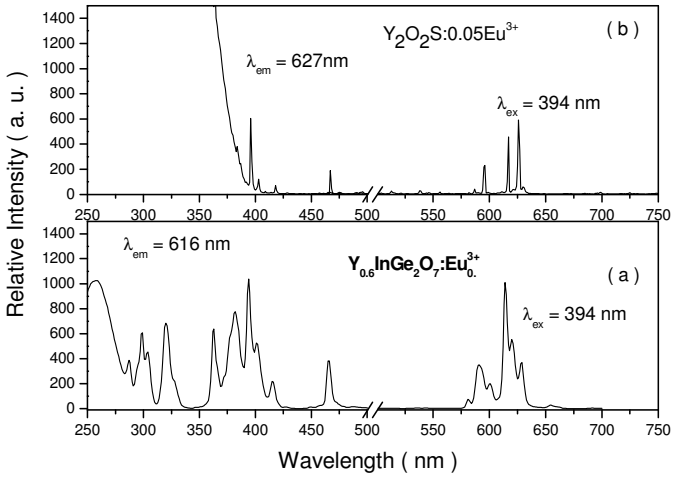

Figure 5. UV excitation and emission (λ_{ex} = 394 nm) spectra of (a) $Y_{0.60}InGe_2O_7:Eu^{3+}{}_{0.40}$ and (b) $Y_2O_2S:0.05Eu^{3+}$ phosphors.

Comparison of the luminescence of $Y_{0.60}InGe_2O_7:Eu^{3+}{}_{0.40}$ and $Y_2O_2S:0.05Eu^{3+}$. Figure 5 shows the near UV excitation and emission spectra of $Y_{0.60}InGe_2O_7:Eu^{3+}{}_{0.40}$ and $Y_2O_2S:0.05Eu^{3+}$. In the excitation spectrum of the phosphor $Y_2O_2S:0.05Eu^{3+}$, the intensity of the charge transfer band is much stronger than that of the *f–f* transitions. The strong broad band before 350 nm corresponds to the Eu-O charge transfer state and the $Eu^{3+}\leftarrow S^{2-}$ charge transfer transition in Y_2O_2S [16]. The relative intensities of the *f–f* transitions of Eu^{3+} are much weaker than those of Eu^{3+} in the phosphor $Y_{0.60}InGe_2O_7:Eu^{3+}{}_{0.40}$. The Eu^{3+} transitions in the excitation spectrum of $Y_{0.60}InGe_2O_7:Eu^{3+}{}_{0.40}$ show more effective absorption in the UV range (394 nm). When the excitation wavelength is 394 nm, the main emission line of $Y_2O_2S:0.05Eu^{3+}$ at 627 nm may also be ascribed to the $^5D_0 \rightarrow {}^7F_2$ transition of Eu^{3+}. Comparing Figures 5a and 5b, the emission

intensity of the phosphor $Y_{0.60}InGe_2O_7:Eu^{3+}_{0.40}$ is approximately 2.8 times higher than that of $Y_2O_2S:0.05Eu^{3+}$ under 394 nm UV irradiation. The CIE chromaticity coordinates of $Y_{0.60}InGe_2O_7:Eu^{3+}_{0.40}$ (x = 0.644, y = 0.356) are close to those of $Y_2O_2S:0.05Eu^{3+}$ (x = 0.645, y = 0.354) because the former are used in LEDs. Thus, $Y_{0.60}InGe_2O_7:Eu^{3+}_{0.40}$ may be an efficient red-emitting phosphor for white LEDs.

CONCLUSIONS

Eu^{3+}-doped $YInGe_2O_7$ phosphors were prepared by a solid-state reaction. Compared with the $Y_2O_2S:0.05Eu^{3+}$ phosphor, the obtained $Y_{0.60}InGe_2O_7:Eu^{3+}_{0.40}$ phosphor showed a stronger excitation band around 400 nm and enhanced red emissions because of Eu^{3+} $f - f$ transitions under 394 nm light excitation. The CIE chromaticity coordinates (x = 0.644, y = 0.356) of the phosphor were close to those of the NTSC standard. All of the results indicated that the red phosphor synthesized in this work is a suitable candidate for the fabrication of near UV InGaN-based LEDs.

ACKNOWLEDGMENTS

This work was financially supported by grants from the National Natural Science Foundation of China (No 61264003); Natural Science Foundation of Guangxi Province (No. 2011GXNSFA018054).

REFERENCES

1. Narendran, N.; Gu, Y.; Freyssinier-Nova, J.P.; Zhu, Y. *Phys. Stat. Sol. (A)* **2005**, 202, R60.
2. Wang, Z.L.; Liang, H.B.; Gong, M.L.; Su, Q. *J. Alloy. Compd*. **2005**, 432, 308.
3. Jang, H.S.; Im, W.B.; Lee, D.C.; Jeon, D.Y.; Kim, S.S. *J. Lumin*. **2007**, 126, 371.
4. Hu, Y.; Zhuang, W.; Ye, H.; Wang, D.; Zhang, S.; Huang, X. *J. Alloy. Comp*. **2005**, 390, 226.
5. Wang, Y.H.; Sun, Y.K.; Zhang, J.C.; Ci, Z.E.; Zhang, Z.Y.; Wang, L. *Physica B* **2008**, 403, 2071.
6. Zhu, C.; Xiao, S.; Ding, J.; Yang, X.; Qiang, R. *Mater. Sci. Eng. B* **2008**, 150, 95.
7. Neeraj, S.; Kijima, N.; Cheetham, A.K. *Chem. Phys. Lett*. **2004**, 387, 2.
8. Boutinaud, P.; Pinel, E.; Dubois, M.; Vink, A.P.; Mahiou, R.J. *Lumin*. **2005**, 111, 69.
9. Chen,g G.; Wei, X.; Cheng, L.; Liu, Q.; Wang, X.; Sun, H.; Zhang, X.; Qiu, G. *Rare Metals* **2011**, 30, 14.
10. Zhang, Q.Y.; Pita, K.;Ye, W.; Que, W.X. *Chem. Phys. Lett*. **2002**, 351, 163.
11. Chang, Y.S.; Lin, H.J.; Chai, Y.L.; Li, Y.C. *J. Alloy. Compd*. **2008**, 460, 421.
12. Chang, Y.S. J. *Electron. Mater*. **2008**, 37, 1024.
13. Ekambaram, S.; Patil, K.C.; Maaza, M. *J. Alloys Compd*. **2005**, 393, 81.
14. Rao, R.P. *Solid State Commun*. **1996**, 99, 439.
15. Wang, L.; Shi, L.; Liao, N.; Jia, H.; Yu, X.; Du, P.; Xi, Z.; Jin, D. *Thin Solid Films* **2010**, 518, 4817.
16. Seo, J.H.; Sohn, S.H. *Mater. Lett*. **2010**, 64, 1264.
17. Reddy, K.R.; Annapurna, K.; Buddhudu, S. *Mater. Res. Bull*. **1996**, 31, 1355.
18. Shionoya, S.; Yen, W.M. *Phosphor Handbook*, *CRC Press*: *Boca Raton*; **1999**; p190.
19. van der Voort, D.; deRijk, J.M.E.; van Doorn, R.; Blasse, G. *Mater. Chem. Phys*. **1992**, 31, 333.
20. Rainho, J.P.; Carlos, L.D.; Rocha, J. *J. Lumin.* **2000**, 87–89, 1083.